Palaeontology
The Palaeontological Association
www.palass.org

[Palaeontology, 2020, pp. 1–11]

SYNCHROTRON X-RAY FLUORESCENCE ANALYSIS REVEALS DIAGENETIC ALTERATION OF FOSSIL MELANOSOME TRACE METAL CHEMISTRY

by CHRISTOPHER S. ROGERS[1,2,*], SAMUEL M. WEBB[3] *and* MARIA E. McNAMARA[1,2,*]

[1]School of Biological, Earth & Environmental Sciences, University College Cork, Distillery Fields, North Mall, Cork, T23 TK30, UK; christopher.rogers@ucc.ie; maria.mcnamara@ucc.ie
[2]Environmental Research Institute, University College Cork, Lee Road, Cork, T23 XE10, Ireland
[3]SLAC National Accelerator Laboratory, Stanford Synchrotron Radiation Lightsource, 2575 Sand Hill Road, Menlo Park, CA 94025, USA
*Corresponding authors

Typescript received 9 December 2019; accepted in revised form 24 July 2020

Abstract: A key feature of the pigment melanin is its high binding affinity for trace metal ions. In modern vertebrates trace metals associated with melanosomes, melanin-rich organelles, can show tissue-specific and taxon-specific distribution patterns. Such signals preserve in fossil melanosomes, informing on the anatomy and phylogenetic affinities of fossil vertebrates. Fossil and modern melanosomes, however, often differ in trace metal chemistry; in particular, melanosomes from fossil vertebrate eyes are depleted in Zn and enriched in Cu relative to their extant counterparts. Whether these chemical differences are biological or taphonomic in origin is unknown, limiting our ability to use melanosome trace metal chemistry to test palaeobiological hypotheses. Here, we use maturation experiments on eye melanosomes from extant vertebrates and synchrotron rapid scan-x-ray fluorescence analysis to show that thermal maturation can dramatically alter melanosome trace element chemistry. In particular, maturation of melanosomes in Cu-rich solutions results in significant depletion of Zn, probably due to low pH and competition effects with Cu. These results confirm fossil melanosome chemistry is susceptible to alteration due to variations in local chemical conditions during diagenesis. Maturation experiments can provide essential data on melanosome chemical taphonomy required for accurate interpretations of preserved chemical signatures in fossils.

Key words: fossil, soft tissue, taphonomy, synchrotron x-ray fluorescence.

MELANIN is an essential biomolecule in animals, that supports immunity (Agius & Roberts 2003; Nappi & Christensen 2005) and facilitates key physiological processes including directional photoreception in the eye (Oakley & Speiser 2015) and the protection of tissues from UV damage (Brenner & Hearing 2007). Melanin may also contribute to metal homeostasis via its high binding affinity for metal ions such as Ca^{+2}, Fe^{+3}, Cu^{+2} and Zn^{+2} (Hong & Simon 2007; Wogelius *et al.* 2011; Rossi *et al.* 2019) (albeit the two common forms of melanin, eumelanin and phaeomelanin, differ in metal affinity) (Wogelius *et al.* 2011; Manning *et al.* 2019). Remarkably, evidence of melanin has been reported from many vertebrate fossils, usually in association with preserved melanosomes (micron-sized organelles) (Lindgren *et al.* 2012; McNamara *et al.* 2016). As with melanin in extant animals (Hong & Simon, 2007, fossil melanin can associate with metals, especially Cu (Wogelius *et al.* 2011) and Zn (Manning *et al.* 2019). Preserved associations between these metals and melanosomes can be tissue and taxon-specific (Rogers *et al.* 2019; Rossi *et al.* 2019), thus offering the potential to inform on the internal anatomy (Rossi *et al.* 2019) and phylogenetic affinities (Rogers *et al.* 2019) of fossils and the functional evolution of melanin (Rossi *et al.* 2019).

The metal inventory of fossil melanin, however, differs from that of modern analogues, even in closely related taxa (Rogers *et al.* 2019; Rossi *et al.* 2019). In the case of vertebrate eye melanosomes, concentrations of Zn are markedly lower in fossils relative to modern vertebrate eyes, and concentrations of Cu and Fe are higher (Rogers *et al.* 2019). The origins of these differences are unclear, thus impacting our ability to confidently interpret preserved melanosome chemistry. Previous work on fossils acknowledged the possibility of diagenetic alteration of the trace metal inventory of melanosomes (Wogelius *et al.* 2011); this is supported by experimental evidence that the trace element chemistry of melanin is sensitive to

doi: 10.1111/pala.12506

fluctuations in pH (Hong & Simon 2007) and high metal concentrations (Chen *et al.* 2009). Characterization of the impact of diagenesis on melanosome trace metal chemistry is therefore essential for identifying taphonomic biases in the melanosome fossil record.

Here, we resolved these issues by conducting maturation experiments on melanosomes from extant vertebrate eyes at elevated pressures and/or temperatures and with different chemical media in order to simulate how different pore fluids (i.e. sources of metal ions) interact with melanosomes during diagenesis. Analysis of the results using synchrotron rapid scan-x-ray fluorescence analysis (SRS–XRF) and x-ray absorption spectroscopy (XAS) reveals which melanosome-associated elements are susceptible to changes in concentration during diagenesis. Critically, the experimental data aid interpretations of the chemical differences between fossil and modern eye melanosomes, thus informing on key biases in the melanosome fossil record.

MATERIAL AND METHOD

Modern specimens

Specimens of European sea bass (*Dicentrarchus labrax* n = 14) were obtained from commercial suppliers and dissected within 24 h after death. One eye from each animal was bisected and melanin was enzymatically extracted from the posterior half of each eye (including the melanosome-rich choroid and retinal pigment epithelium (RPE)) using the method in Rossi *et al.* (2019). The extraction process breaks down cellular material and can degrade phaeomelanin, yielding extracts that are biased towards eumelanin (Liu *et al.* 2005).

Fossil specimens

Preserved melanosomes from the eyespot of a specimen of *Dapalis macrurus* (CKGM F 6427; Actinopterygii, Perciformes; from Alpes de Haute-Provence, France (Oligocene)) and eyespots from the fossil teleosts Tetradontiformes indet. (NHMD 199838; from the Fur Formation, Denmark (Eocene)) and *Knightia* (FOBU 17591; Actinopterygii, Clupeiformes; from the Fossil Butte member of the Green River formation, Colorado/Utah/Wyoming (Eocene)) were reported in Rogers *et al.* (2019) and analysed further as below.

The respective fossil localities vary in lithology and diagenetic history. NHMD 199838 is hosted in diatomite that was deposited in a restricted marine basin (Pedersen & Buchardt, 1996) and experienced at least 40–45°C and ~33–49 bar during diagenesis (McNamara *et al.* 2013). FOBU 17591 is hosted in laminated limestone that was deposited in a restricted terrestrial basin with marked salinity fluctuations during deposition (Loewen & Buchheim 1998). Data on diagenetic history are not available for the Fossil Butte Member (part of the Fossil Basin); sediments from the Uinta Basin of the Green River Formation experienced burial conditions of up to 65–180°C and ~400–2000 bar (McNamara *et al.* 2013). CKGM F 6427 is preserved in a laminated limestone but lacks stratigraphic data; specimens of this taxon are common in the freshwater/brackish lacustrine limestones of the Campagne–Calavon Formation of Alpes de Haute-Provence (Gaudant, 2015), though data on burial history are not available.

Institutional abbreviations. CKGM, Cork Geological Museum at University College Cork, Ireland; FOBU, Fossil Butte National Monument, Wyoming, USA; NHMD, Natural History Museum of Denmark, Copenhagen, Denmark.

EDTA treatment of melanin

Unmatured melanin (50–100 mg) extracted from a single *Dicentrarchus* eye was added to an aqueous solution of EDTA (1 ml) for 24 h at room temperature and then centrifuged. This process was repeated six times followed by washing four times in biomolecular-grade water in order to remove excess EDTA. The EDTA-treated extract was then added to 1 ml of 16 mmol Cu-solution for 24 h at room temperature before being washed twice in 10^{-3} M HCl to precipitate any Cu still in solution (Hong *et al.* 2004). The extract was washed twice in biomolecular water and once in acetone. Half of the extract was experimentally matured (see below).

Experimental maturation

Taphonomic studies investigating the impact of maturation on soft tissues typically use elevated temperatures and pressures for relatively short periods of time (usually < 24 h) to artificially simulate aspects of the maturation process (McNamara *et al.* 2013; Colleary *et al.* 2015). Such experiments are known to yield morphological and chemical phenomena similar to those exhibited by fossils (Stankiewicz *et al.* 2000). Melanosome extracts for experimental maturation (n = 12) were each inserted into separate Au capsules. To each capsule was added 1 ml of experimental medium, defined as follows. The EDTA-treated extract used distilled deionized (DD) water. All other extracts used either DD water, 'Cu-solution' (*Trace*CERT copper standard for atomic absorption spectroscopy (AAS); 1000 mg/l), 'Zn-solution' (*Trace*CERT zinc standard for AAS; 1000 mg/l) or 'Cu–Zn-solution'

(50:50 mixture of *Trace*CERT copper and zinc standards for AAS; Rogers *et al.* 2020, table S1). The inclusion of metal ion solution in some experiments is designed to test how variation in diagenetic pore fluid chemistry impacts melanin chemistry. All metal ion solutions have a concentration of 16 mmol and are at pH 3.

Brushes were used to remove any extract or experimental medium from the termini of each capsule prior to them being welded shut with a Lampert PUK 4 microwelding system. Sealed capsules were thermally matured for 24 h at 200°C in either an oven at one bar or, for some samples (including EDTA-treated extracts) a custom-built high-pressure high-temperature rig (StrataTech, UK) at 120 bar. It was not possible to measure the pH of the experimental medium at the end of the experiment due to the small size of the capsules and unpredictable escape of fluid from the capsules upon opening.

Synchrotron rapid scanning x-ray fluorescence (SRS–XRF) analysis

X-ray fluorescence spectra were collected from matured and untreated extracts and fossils at beamline 2-3 at the Stanford Synchrotron Radiation Lightsource (SSRL). Extracts and small samples (*c.* 1 mm^2) of dark brown carbonaceous material from the eyespot of the fossil fish *Dapalis macrurus* (Oligocene; CKGM F 6427) were mounted on kapton tape. Samples were spatially rastered by a microfocused beam of 2 μm^2 provided by an Rh-coated Kirkpatrick–Baez mirror pair with 20–50 ms/pixel dwell time. A Si (111) double crystal monochromator was used to set incident x-ray energy at 11 keV; the storage ring was in top-off mode at 3 GeV and contained 500 mA. Samples were mounted at 45° to the incident x-ray and the intensity of the beam was measured using a nitrogen-filled ion chamber. At each data point, the intensity of fluorescence lines for selected elements (P, S, Ca, Ti, Mn, Fe, Ni, Cu and Zn) was collected and monitored using an Xpsress3 pulse processing system (Quantum Detectors) coupled to a silicon drift Vortex detector (Hitachi, USA) for energy discrimination.

SRS–XRF data processing

MicroAnalysis Toolkit software (Webb 2011) was used to normalize fluorescence spectra and calibrate concentrations of each element in $\mu g/cm^2$ against NIST traceable thin-film elemental standards. Mean concentrations and standard deviation values for each element were calculated for selected regions of interest. Inspection of SRS–XRF spectra from the multi-channel analyser (MCA) data reveals that in extracts the concentrations of certain elements (P, S, Ti and Mn) are too low to be discriminated confidently from the background (Rogers *et al.* 2020, figs S1–S7). Concentration data from these elements were therefore excluded from further analyses. Ni was identified in the MCA data but concentrations (<9 $\mu g/cm^2$) were markedly lower than those of other elements and thus Ni was also excluded from further analysis.

The SRS–XRF data were analysed further using linear discriminant analysis (LDA) in PAST (Hammer *et al.* 2001) to visualize variations in the chemistry of selected elements (Ca, Fe, Cu and Zn) among the melanin extracts and fossil melanosomes. The significance of differences in concentration among samples was assessed using ANOVA or non-parametric alternatives (Kruskal–Wallis and Welch's F-test) and appropriate pairwise post hoc analyses (Tukey, Mann Whitney and Dunn, respectively). Differences in elemental concentrations among extracts were visualized using box plots.

X-ray absorption spectroscopy (XAS)

EDTA-treated extracts and samples from the eyespot of *Dapalis* were mapped at beamlines 2-3 and 10-2 at the Stanford Synchrotron Radiation Lightsource (SSRL). At beamline 2-3, extracts were analysed as above. At beamline 10-2, extracts were analysed using a 25–200 μm beam using a series of tungsten apertures. Four to six points of interest were selected from each SRS–XRF map. XAS spectra were collected from these points by driving the emitted intensity from ~8787 to ~9827 eV across the Cu K edge (set at 8987 eV using a Cu foil) in a stepwise fashion (step size of 10 eV from 8749 to 8958 eV, except for between 8959 and 9006 eV (i.e. across the Cu K edge) where step size of 0.35 eV was used. Between two and seven repeat scans (15 min each) were collected at each point.

A Cu foil was used to calibrate the energy of the monochromator. X-ray absorption near edge structure spectroscopy (XANES) was used to investigate the oxidation state of Cu associated with the melanosomes in our dataset. Each spectrum was monitored for loss of intensity and photo-reduction associated with exposure to the electron beam. No evidence for photo-reduction was observed among replicate scans and repeat scans at each point are mutually consistent. Spectra were processed as standard (i.e. via normalization and background removal) in Athena (Ravel & Newville 2005).

RESULTS

Trace metal concentrations in matured melanosome extracts

Linear discriminant analysis (LDA) plots of the SRS–XRF data show extensive overlap of data from unmatured and

matured melanosomes in chemospace (Fig. 1A, B). Differences in trace element chemistry between untreated extracts and extracts experimentally matured in DD water are not statistically significant (p-values = 0.1034–0.8206; Rogers *et al.* 2020, table S2A–C); these two samples cannot therefore be distinguished chemically.

Concentrations of Ca (Welch F: df = 16.18, F = 73.39, $p = 7.91^{-11}$) and Cu (df = 17.47, F = 118.8, $p = 5.792^{-13}$) are significantly different between unmatured extracts and extracts matured in Cu and/or Zn-solutions (Fig. 2; Rogers *et al.* 2020; table S2A). More specifically, concentrations of Ca are significantly lower in extracts matured in Zn-solution and mixed Cu–Zn-solution (Dunn's *post hoc*: p = 0.002–0.006). Concentrations of Cu are higher in extracts matured in Cu-solution and mixed Cu–Zn-solution (p = 0.001–0.002; Rogers *et al.* 2020, table S2B–C). Concentrations of Zn are significantly lower in all extracts matured with Cu-solution and/or Zn-solution (Kruskal–Wallis H: $\chi^2 = 23.33$, $p = 0.001$; Dunn's *post hoc*: p = 0.001–0.006). Variations in Fe concentrations among untreated and experimentally matured extracts are not significant (ANOVA: df = 2.115, F = 17.5, $p = 0.1034$).

Comparison with fossil trace element chemistry

The principal component analysis plot of the fossil data reveals that the eyespot data for individual specimens plot close to the data for the associated host sediment (Rogers *et al.* 2020, fig. S9); the data for individual specimens and their sediment do not overlap with those for other fossils. Variation in concentrations of Ca, Fe and Cu among specimens are significantly different (Ca: Welch F: df = 2.668, F = 37.62, $p = 0.01109$; Fe: ANOVA: df = 8, F = 162, $p = 6.01^{-06}$; Cu: Welch F: df = 2.983, F = 13.7, $p = 0.03136$; *posthoc* tests: Rogers *et al.* 2020, table S4). Concentrations of Zn do not differ significantly among specimens (Kruskal–Wallis H: $\chi^2 = 0.3556$, $p = 0.8371$).

Differences in concentrations of Cu between the fossil eyespots and the host sediment are significantly different for each fossil specimen (Rogers *et al.* 2020, table S4). In addition, concentrations of Fe (and, in *Dapalis*, Ca) are significantly different between the eyespot of *Knightia* and the respective host sediment; similarly, concentrations of Fe and Ca differ significantly between the eye of *Dapalis* and the host sediment. Differences in concentrations of

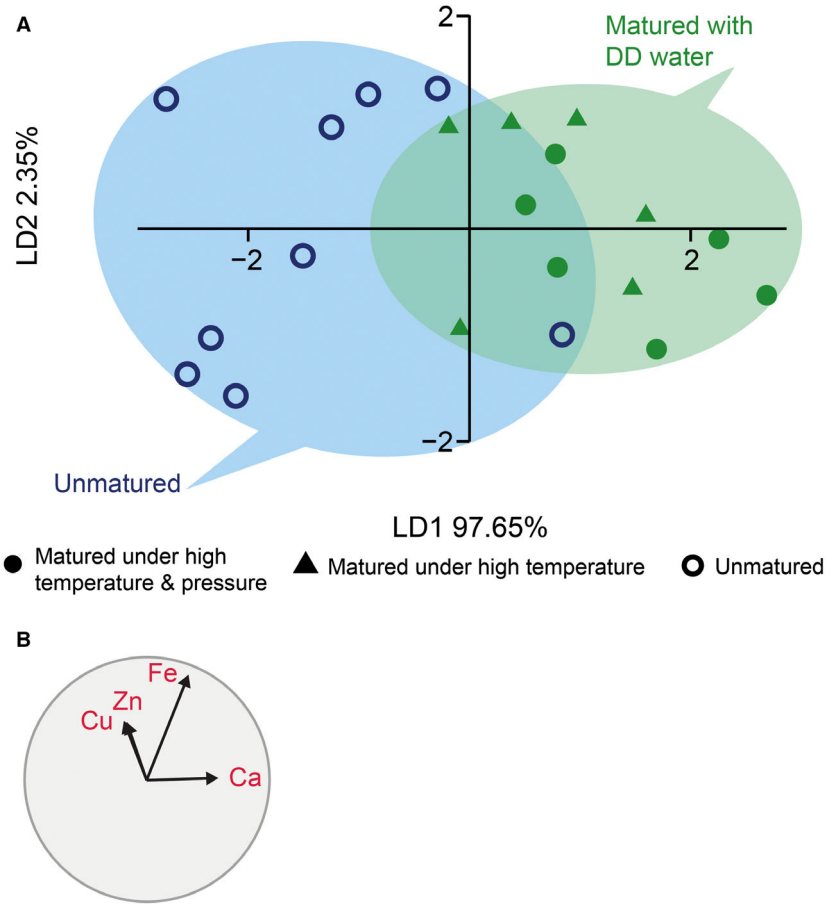

FIG. 1. Effect of temperature and pressure on the trace element chemistry of eye melanosomes of *Dicentrarchus* (Actinopterygii, Perciformes). A, linear discriminant analysis chemospace plot based on measured concentrations of Ca, Fe, Cu and Zn in untreated and experimentally matured melanosomes. B, biplot showing the contribution of each element to variation in A.

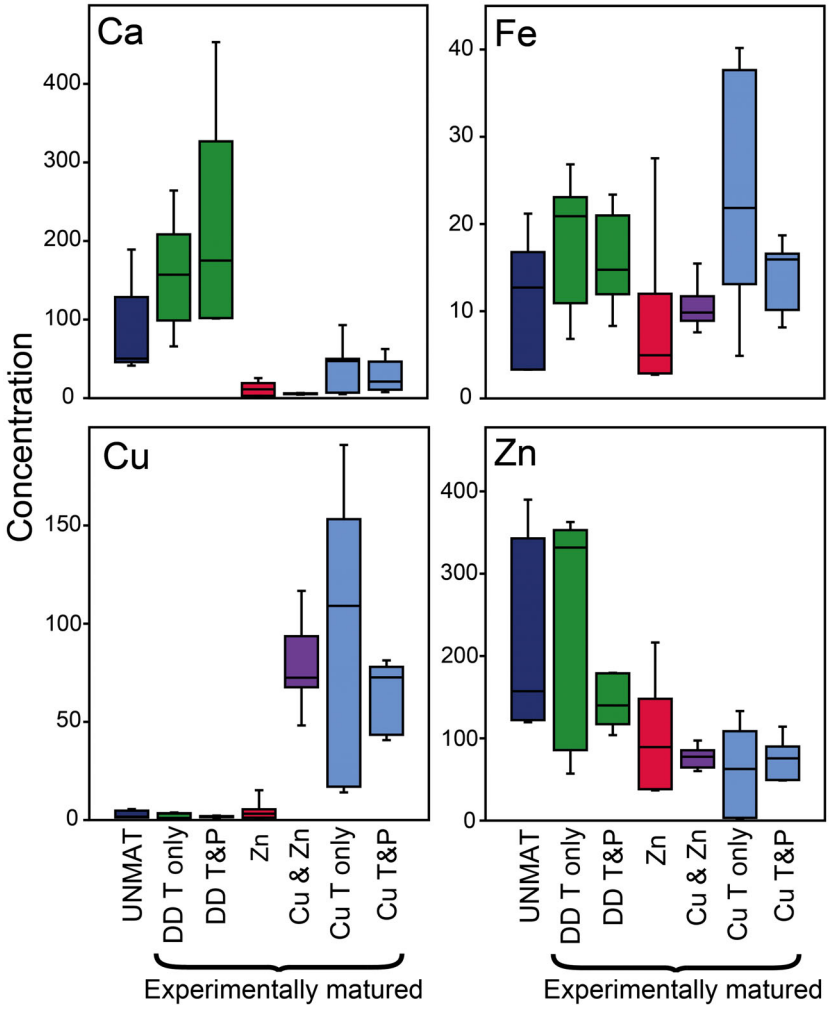

FIG. 2. Differences in the concentrations of key elements Ca, Fe, Cu and Zn in melanosome extracts from eyes of *Dicentrarchus*. X-axis labels refer to untreated extracts (UNMAT) and extracts matured under various conditions as follows: Cu T only, Cu-solution with elevated temperature; Cu T&P, Cu-solution with elevated temperature and pressure; Cu & Zn, Cu–Zn-solution with elevated temperature and pressure; DD T only, distilled water with elevated temperature; DD T&P, distilled water with elevated temperature and pressure; Zn, Zn-solution with elevated temperature and pressure. Concentration units are μg/cm^2.

Zn between eyespots and host sediment are not significantly different for any of the three fossils analysed (Rogers *et al.* 2020, table S4).

LDA plots of the total dataset reveal three major groupings in the LDA chemospace (Fig. 3A): (1) fossil melanosomes; (2) melanosome extracts matured in Cu-solution and Cu–Zn-solution; and (3) melanosome extracts matured in DD water, in Zn-solution and untreated melanosomes. The primary elements driving this chemical variation are Ca, Cu and Zn (Fig. 3B); in particular, fossil melanosomes have significantly lower concentrations of Zn than untreated modern equivalents (Kruskal–Wallis H: $\chi^2 = 12.79$, $p = 0.0003$). Fossil and untreated modern melanosomes do not differ significantly in concentrations of Ca (Kruskal–Wallis H: $\chi^2 = 1.421$, $p = 0.233$), Cu (H: $\chi^2 = 0.002$, $p = 0.965$) or Fe (ANOVA: df = 17, F = 3.478, $p = 0.081$) (Rogers *et al.* 2020; table S5). In the total dataset, however, differences in Cu concentrations between samples are significant (Kruskal–Wallis H: $\chi^2 = 7.2$, $p = 0.02732$); differences in concentrations of Ca ($\chi^2 = 5.422$, $p = 0.06646$), Fe ($\chi^2 = 5.6$, $p = 0.06081$) and Zn ($\chi^2 = 0.3556$, $p = 0.8371$) are not significant.

Cu-XANES spectra for all samples analysed have a dominant peak centred at 8997.5 ± 1 eV showing a major contribution from Cu(II) (Fig. 3C). Only the Cu-XANES profile from the eyespot of *D. macrurus* shows a distinct pre-edge feature at 8984.5 eV, indicating a contribution from Cu(I).

DISCUSSION

The results of our study reveal that the metal inventory of eye melanosomes is not significantly altered by maturation in DD water (Fig. 1A, B). This suggests that melanosome–metal associations should persist in natural diagenetic scenarios where pore fluids have low concentrations of metal ions and, since pH decreases with increasing temperature, where pH does not vary markedly. In contrast, melanosome extracts matured in Cu

and/or Zn solutions differ in chemistry to untreated samples, and to each other. This confirms that the metal inventory of melanosomes is highly sensitive to local ionic concentrations during diagenesis.

Metals commonly bind to three functional groups within the eumelanin molecule (OH^-, NH_4^+ and $COOH^-$) (Hong *et al.* 2004); Cu can also be accommodated within the eumelanin porphyrin structure, which may survive diagenesis in at least some fossils (Wogelius *et al.* 2011). In *Sepia* melanin, Fe(III) can bind to NH_4^+ or OH^- (Hong *et al.* 2004); Ca(II) and Zn(II) bind to $COOH^-$ and Cu(II) binds primarily to OH^-. In all cases eumelanin-bound metals are strictly co-ordinated to light elements (i.e. O/N). Unlike eumelanin, phaeomelanin comprises monomers (benzothiazine and benzothiazole) that contain S and can chelate Zn (Manning *et al.* 2019); whether the phaeomelanin S-groups (and other groups present, e.g. NH^-) commonly bind other metals is unclear.

Extracts matured in Cu-solution are enriched in Cu and depleted in Zn relative to unmatured melanosomes. Experiments at room temperature and pressure indicate that where Cu concentrations exceed 10 mmol, additional Cu(II) can bind to $COOH^-$ sites normally occupied by Ca(II) and Zn(II) (Hong & Simon 2006), displacing the latter two elements. This is consistent with evidence of Cu-binding to melanin $COOH^-$ groups in fossil feathers (Wogelius *et al.* 2011). In our experiments it is possible that the concentration of the Cu-solutions used (16 mmol) was sufficiently high to trigger replacement of Zn(II) by Cu(II) at $COOH^-$ sites during maturation. Experiments on artificial eumelanin, however, show a decrease in $COOH^-$ with thermal maturation (Ito *et al.* 2013). Elevated Cu concentrations in our experiments may therefore reflect (at least in part) the binding of Cu to unoccupied OH^- or NH_4^+ rather than $COOH^-$.

Surprisingly, Zn concentrations decrease even when melanosome extracts are matured in solutions containing Zn. Following saturation of $COOH^-$ groups with Zn(II), NH_4^+ and OH^- groups can present secondary binding sites for Zn(II) (Hong & Simon 2006). Melanin, however, has a much higher overall binding affinity for Cu(II) than for Zn(II) (Hong & Simon 2007) and thus Zn(II) may be unable to bind to OH^- groups in melanin when they are already occupied by Cu(II). Low Zn concentrations in melanosomes matured in Cu–Zn-solutions may therefore reflect the following: (1) saturation of OH^- groups by Cu (II) from the experimental medium and the inability of Zn(II) to displace melanin-bound Cu(II) at these sites; and (2) a decrease in the abundance of $COOH^-$ bonds due to thermal maturation (Ito *et al.* 2013).

The decrease in Zn concentrations in melanosomes matured in Zn-solutions (i.e. where saturation of OH^- groups by Cu(II) cannot occur, as in experiments with Cu-solution) is also consistent with a maturation-induced decrease in available $COOH^-$ (Ito *et al.* 2013). This indicates that the original $COOH^-$–Zn bond present in the untreated extracts was unstable under the conditions used in our experiments.

Concentrations of Fe do not differ among untreated and treated melanosomes. This is somewhat surprising because melanin has a higher affinity for Cu(II) than Fe (III) (Hong & Simon, 2007) and thus Cu(II) may be expected to replace Fe(III) at the OH^- group (to which Cu commonly binds; Hong & Simon 2007) and the NH_4^+ group (to which it binds when present in concentrations < 10 mmol; Hong & Simon 2006). Instead, our data suggest that the additional Cu(II) has not displaced Fe(III) at OH^- and NH_4^+ groups but is bound elsewhere, either to unoccupied functional groups or to $COOH^-$ groups in which Cu(II) replaces previously bound metals such as Zn(II).

Patterns of Ca enrichment and depletion in our dataset are complex. Relative to untreated samples, melanosome extracts are depleted in Ca when matured in Zn and Cu–Zn-solutions but concentrations of Ca are the same when extracts are matured in Cu-solution (Fig. 2). This may reflect changes in pH during the experiments. Metal binding sites in *Sepia* melanin are sensitive to changes in pH; more specifically, increased acidity (e.g. a change from pH 7 to pH 2) results in a decrease in the concentration of elements bound to $COOH^-$ groups (Liu *et al.* 2004). This reflects protonation of $COOH^-$ groups by H^+ and associated replacement of chelated metals such as Ca(II) (Liu *et al.* 2004). The exact reasons why this occurs in melanosome extracts matured with Zn and Cu–Zn-solutions but not in extracts matured only in Cu solutions is unclear but it may reflect differences in temporal changes in pH evolution in different experimental settings.

The suspension of melanin in low pH Cu and/or Zn-solutions in our experiments may have resulted in the replacement of $COOH^-$-bound Ca(II) and Zn(II) by H^+. This process cannot, however, explain the high Ca concentrations in extracts matured in Cu-solution, the origin of which remains unclear. The persistence of Ca(II) in thermally matured samples implies either the survival of some $COOH^-$ groups under conditions understood to induce decarboxylation (Ito *et al.* 2013) or binding of Ca (II) to other functional groups in melanin or associated proteins within the melanosome. It is possible that the Ca signal could reflect contributions from other recalcitrant tissue components of the eye, but this is unlikely given that the extracts comprise near-pure agglomerations of melanosomes.

Our experiments provide an empirical basis for interpreting the chemistry of fossil melanosomes and, in particular, can help us interpret key chemical differences

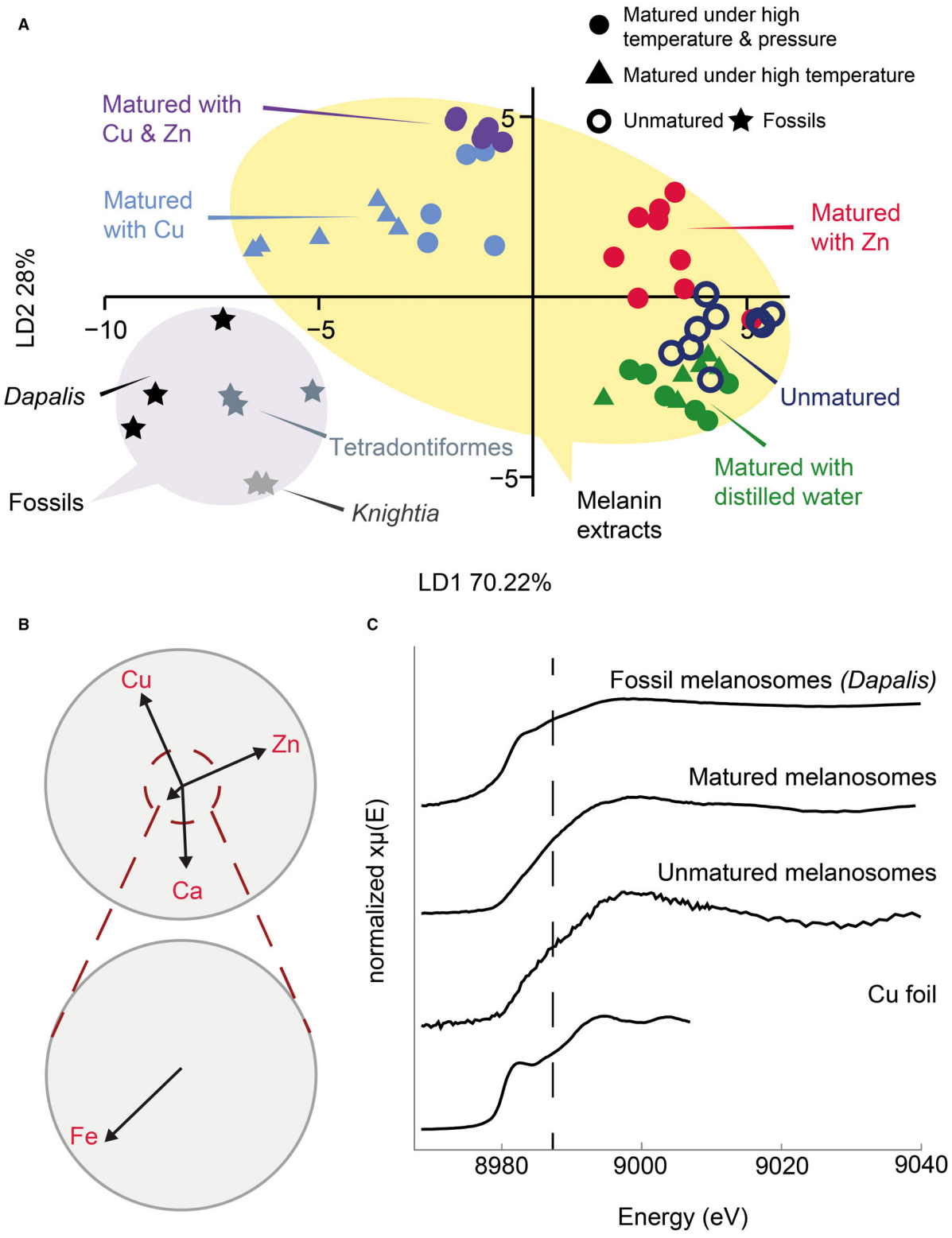

FIG. 3. Comparison of the trace element chemistry of melanosome extracts and fossil melanosomes. A, linear discriminant analysis chemospace plot including data for Ca, Fe, Cu and Zn in unmatured and matured melanin extracts from eye melanosomes of *Dicentrarchus* and from fossil Teleostei (*Dapalis*, *Knightia* and Tetradontiformes). B, biplot of key elements and their contribution to variation in A. C, XANES spectra at the Cu K edge at 8987 eV (dashed line).

between these and modern melanosomes. Differences in chemistry between the fossil specimens studied may reflect taxonomic or biota-level differences; the small sample size prevents discrimination of these interpretations. Given other evidence for pervasive biota-level control on fossil melanosome chemistry (Rossi *et al.* 2020), the chemical differences among the specimens in this study probably represent a sedimentary signal (Rogers *et al.* 2020, fig. S9). The consistent offset in the chemical data for eyespots (especially enrichment of Cu) relative to the host sediment could indicate retention of a component of original chemistry (i.e. naturally elevated concentrations of Cu similar to those *in vivo*) or concentration of elements, especially Cu, in fossil melanosomes during diagenesis.

Direct comparison of the fossil and experimental data reveal that both fossil and thermally matured melanosomes are strongly depleted in Zn relative to unmatured samples. This supports our experimental data on Zn mobility during diagenesis and suggests that the Zn concentrations in the fossils are not original but probably lower than *in vivo*. In natural settings, any Zn(II) displaced as a result of a decrease in pH is likely to be mobilized and lost from the system. Alternatively, displaced Zn may be rendered unavailable for re-chelation by fossil melanin via incorporation into inorganic mineral precipitates in the host sediment.

A decrease in pH could occur relatively early *post mortem* via the release of organic acids during decay (Briggs & Kear 1993) or through contact with pore waters rich in H^+ ions. Higher temperatures at deeper burial conditions would also lower pH, further promoting the loss of Zn from fossil melanosomes. Degradation of phaeomelanin (and loss of key Zn binding sites including S^{2-} and OH^-; Manning *et al.* 2019) during diagenesis could lead to a further depletion of Zn. This process is unlikely to contribute significantly to our experimental data, however, as the eye melanin of *D. labrax* is dominated by eumelanin *in vivo* (Rogers *et al.* 2019) and most or all phaeomelanin originally present in the tissue is likely to have been degraded during enzymatic extraction (Liu *et al.* 2005). Uplift and exposure would presumably result in an increase in local pH, but it is unclear whether thermally altered melanin could bind available Zn in this scenario, especially given that thermal maturation is associated with decarboxylation of melanin (Ito *et al.* 2013) and thus loss of preferred functional groups for Zn-melanin chelation.

Ca, Fe and Cu concentrations are similar in fossil melanosomes and unmatured extracts. This suggests that original associations between Ca(II), Fe(III) and Cu(II) and melanin may have been retained. Melanin, however, has a lower binding affinity for Ca(II) than Zn(II) (Hong & Simon 2007); given that Zn was lost from matured melanosomes in our experiments it thus seems unlikely that original associations between Ca(II) and melanin would survive diagenesis. Instead, it is plausible that Ca concentrations in the matured melanosome extracts may reflect loss early during diagenesis and subsequent re-binding of Ca(II) once local pH and ionic conditions become more favourable. This suggests that the melanin molecule may retain a dynamic relationship with its environment long into diagenesis. Other metals such as Fe and Cu, originally bound to melanin, could also be lost and rebound in this fashion. Alternatively, some Ca, Fe and Cu associated with fossil eye melanosomes may have been bound to non-melanin labile organic components *in vivo*. Breakdown of those compounds during diagenesis and subsequent incorporation of metal ions into remnants of the melanin molecule (Wogelius *et al.* 2011) could contribute to concentrations of these metals in fossil melanosomes, but this hypothesis requires testing. Although biomolecules are understood to undergo the loss of functional groups during diagenesis (Eglington & Logan 1991; Ito *et al.* 2013), our results suggest at least some of these functional groups must survive this process and remain viable binding sites for various metal ions.

Application of these SRS–XRF data to fossils strongly suggests that low Zn concentrations and low Zn:Cu ratios in some fossil vertebrate eye melanosomes are a diagenetic artefact (Fig. 4). Our previous study revealed that eye melanosomes in fossil vertebrates have low Zn relative to extant analogues (Rogers *et al.* 2019). Our experimental data reveal that this probably reflects the loss of Zn and/or the replacement of Zn by Cu during diagenesis. Variation in the chemistry of melanosomes preserved in fossils from different biotas probably reflects different ionic concentrations, pH and burial regimes during diagenesis (Rogers *et al.* 2019). Variation in diagenetic regime, however, is less likely to explain spatial heterogeneity in melanin chemistry within a single fossil. In the latter scenario chemical variation is more likely to reflect biological factors, such as original variation in eumelanin and phaeomelanin content due to integumentary patterning (Wogelius *et al.* 2011) and/or enrichment in various internal organs (Rossi *et al.* 2019, 2020). Higher concentrations in some fossil vertebrates, especially those hosted within concretions (such as those from the Mazon Creek), may reflect rapid cementation of the host sediment, limiting interactions of pore fluids with melanosomes (and thus loss of Cu and Zn) later during diagenesis.

Cu-XANES spectra for matured and untreated melanosomes are dominated by signals for Cu(II). The local binding environment of melanosomal Cu clearly does not alter substantially during maturation (Fig. 3C). The presence of a Cu(I) signal in fossil melanosomes from *Dapalis* could reflect an artefact of the XANES analysis whereby some Cu(II) was reduced during analysis. Other

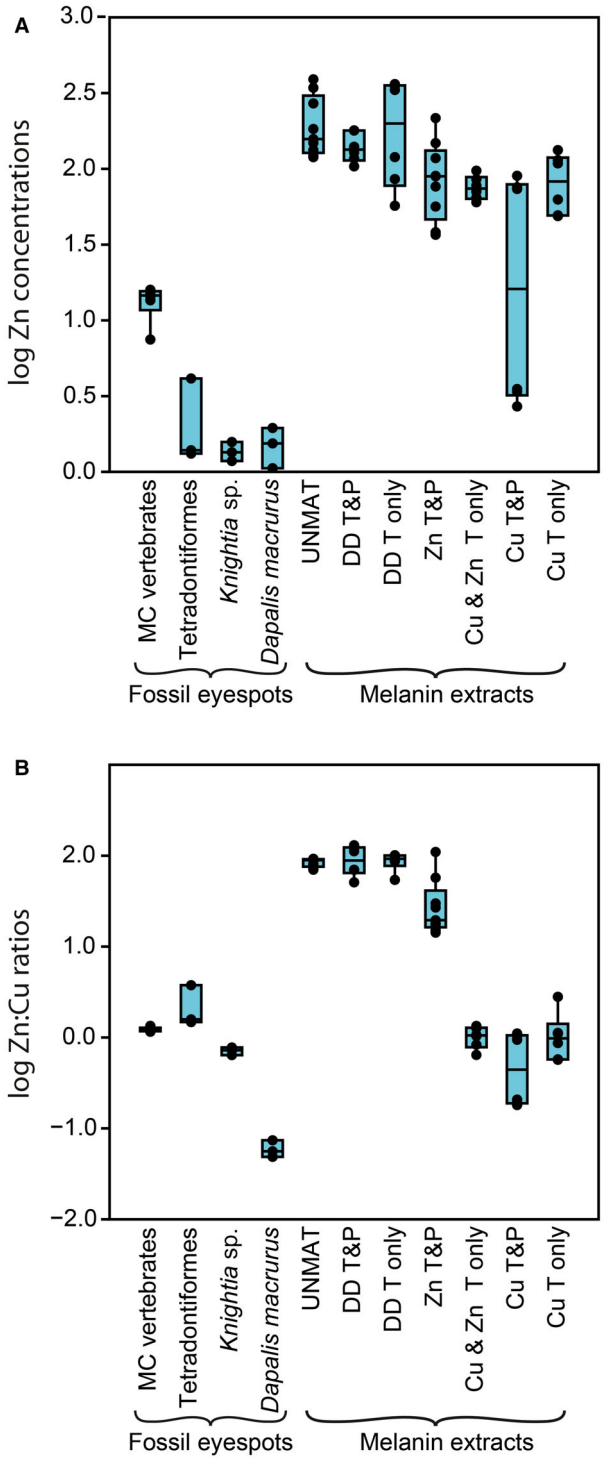

FIG. 4. Comparison of Zn and Cu chemistry data among matured and unmatured melanosome extracts and fossil eyespot melanins: A, log Zn concentrations; B, log Zn:Cu ratios. X-axis labels refer to fossil specimens, untreated extracts (UNMAT) and extracts matured under various conditions as follows: Cu T only, Cu-solution with elevated temperature; Cu T&P, Cu-solution with elevated temperature and pressure; Cu & Zn, Cu–Zn-solution with elevated temperature and pressure; DD T only, distilled water with elevated temperature; DD T&P, distilled water with elevated temperature and pressure; Zn, Zn-solution with elevated temperature and pressure. Data from Mazon Creek (MC) vertebrates, Tetradontiformes and *Knightia* are from Rogers *et al.* (2019). Concentration units are $\mu g/cm^2$.

vertebrate fossils (Wogelius *et al.* 2011; Rogers *et al.* 2019) and modern melanosomes analysed under identical conditions, however, do not show a contribution from Cu(I). Instead, the Cu(I) contribution to the *Dapalis* XANES spectrum may be a real signal, reflecting local conditions during diagenesis.

In conclusion, our study reveals the effects of diagenesis on trace element chemistry of melanosomes. Specifically, our data confirm that relatively low concentrations of Zn in fossil vertebrate eye melanosomes is likely to be a diagenetic feature and that this depletion in Zn relative to modern eye melanosomes is controlled, in large part, by local ionic and pH conditions during diagenesis and not by elevated temperatures and pressures alone. Our experiments also show that original concentrations of Ca and Cu in melanosomes are susceptible to changes during maturation. The fossils we studied show considerable variation in the concentrations of Ca and Cu, probably due to variations in the diagenetic history of the deposit. Our data also reveal that the oxidation state of Cu is not altered under conditions of our maturation experiments, but that it may be altered during fossilization. These results confirm that components of the preserved trace element chemistry of fossil melanosomes could be a diagenetic artefact and that maturation experiments can yield essential insights into the chemical taphonomy of melanosomes that should be incorporated into future interpretations of preserved chemical signatures in fossils.

Collectively, our data emphasize the dynamic nature of links between fossil chemistry and the host sediment, in particular variations in pore fluid chemistry, through time. Melanin elemental chemistry is clearly plastic during diagenesis. Other, more labile, components of fossil chemistry, such as proteins (Asara *et al.* 2007; Schweitzer *et al.* 2007; Schweitzer *et al.* 2013; Schroeter *et al.* 2017) and nucleic acids (Schweitzer *et al.* 2013; Bailleul *et al.* 2020), would presumably be equally, if not more, susceptible to alteration during decay and diagenesis.

Acknowledgements. We thank Nick Edwards and Sharon Bone for XAS and XRF support, T. Clements, T. Slater, V. Rossi for help with XAS and XRF data acquisition and helpful discussion. Supported by European Research Council Starting Grant ERC-2014-StG-637691-ANICOLEVO (to MEM). The use of the Stanford Synchrotron Radiation Lightsource, SLAC National Accelerator Laboratory, is supported by the US Department of Energy, Office of Science, Office of Basic Energy Sciences under contract

no. DE-AC02-76SF00515 via beamtime proposals 4615 and 5072 awarded to MEM. We would like to thank R. A. Wogelius and an anonymous referee for their helpful and constructive reviews of the manuscript.

Author contributions. MEM and CSR conceived the study; CSR, MEM and SMW performed synchrotron rapid scanning-x-ray fluorescence and x-ray absorption spectroscopy (XAS); CSR and MEM. wrote the manuscript with input from SMW.

DATA ARCHIVING STATEMENT

All data is provided in the main text or via the Dryad Digital Repository: https://doi.org/10.5061/dryad.r7sqv9s7q

Editor. Robert Sansom

REFERENCES

AGIUS, C. and ROBERTS, R. J. 2003. Melano-macrophage centres and their role in fish pathology. *Journal of Fish Diseases*, **26**, 499–509.

ASARA, J. M., SCHWEITZER, M. H., FREIMARK, L. M., PHILLIPS, M. and CANTLEY, C. L. 2007. Protein sequences from mastodon and *Tyrannosaurus rex* revealed by mass spectrometry. *Science*, **316**, 280–285.

BAILLEUL, A. M., ZHENG, W., HORNER, J. R., HALL, B. K., HOLLIDAY, C. M. and SCHWEITZER, M. H. 2020. Evidence of proteins, chromosomes and chemical markers of DNA in exceptionally preserved dinosaur cartilage. *National Science Review*, **7**, 815–822.

BRENNER, M. and HEARING, V. J. 2007. The protective role of melanin against UV damage in human skin. *Photochemistry & Photobiology*, **84**, 539–549.

BRIGGS, D. E. G. and KEAR, A. J. 1993. Fossilization of soft tissue in the laboratory. *Science*, **259**, 1439–1442.

CHEN, S., XUE, C., WANG, J., FENG, H., WANG, Y., MA, Q. and WANG, D. 2009. Adsorption of Pb(II) and Cd (II) by squid *Ommastrephes bartrami* melanin. *Bioinorganic Chemistry & Applications*, **2009**, 901563.

COLLEARY, C., DOLOCAN, A., GARDNER, J., SINGH, S., WUTTKE, M., RABENSTEIN, R., HABERSETZER, J., SCHAAL, S., FESEHA, M., CLEMENS, M., JACOBS, B. F., CURRANO, E. D., JACOBS, L. L., LYNG SYLVESTERSEN, R., GABBOTT, S. E. and VINTHER, J. 2015. Chemical, experimental and morphological evidence for diagenetically altered melanin in exceptionally preserved fossils. *Proceedings of the National Academy of Sciences*, **112**, 12592–12597.

EGLINGTON, G. and LOGAN, G. A. 1991. Molecular preservation. *Philosophical Transactions of the Royal Society B*, **333**, 315–328.

GAUDANT, J. 2015. Présence du genre *Lepidocottus* Sauvage, 1875 (Teleostei, Gobioidei) dans l'Oligocène inférieur des environs de Céreste (Alpes-de-Haute-Provence, France). *Geodiversitas*, **37**, 229–235.

HAMMER, Ø., HARPER, D. A. T. and RYAN, P. D. 2001. PAST: Paleontological statistics software package for education and data analysis. *Palaeontologica Electronica*, **4**, 9.

HONG, L. and SIMON, J. D. 2006. Insight into the binding of divalent cations to *Sepia* eumelanin from IR absorption spectroscopy. *Photochemistry & Photobiology*, **82**, 1265–1269.

—— —— 2007. Current understanding of the binding site, capacity, affinity, and biological significance of metals in melanin. *Journal of Physical Chemistry B*, **111**, 7938–7947.

—— LIU, Y. and SIMON, J. D. 2004. Binding of metal ions to melanin and their effects on the aerobic reactivity. *Photochemistry & Photobiology*, **80**, 477–481.

ITO, S., WAKAMATSU, K., GLASS, K. and SIMON, J. D. 2013. High-performance liquid chromatography estimation of cross-linking of dihydroxyindole moiety in eumelanin. *Analytical Biochemistry*, **434**, 221–225.

LINDGREN, J., UVDAL, P., SJÖVDALL, P., NILSSON, D. E., ENGDAHL, A., SCHULTZ, B. P. and THIEL, V. 2012. Molecular preservation of the pigment melanin in fossil melanosomes. *Nature Communications*, **3**, 824.

LIU, Y., HONG, L., KEMPF, V. R., WAKAMATSU, K., ITO, S. and SIMON, J. D. 2004. Ion-exchange and adsorption of Fe(III) by *Sepia* melanin. *Pigment Cell Research*, **17**, 262–269.

—— —— WAKAMATSU, K., ITO, S., ADHYARU, B., CHENG, C. Y., BOWERS, C. R. and SIMON, J. D. 2005. Comparison of structural and chemical properties of black and red human hair melanosomes. *Photochemistry & Photobiology*, **18**, 135–144.

LOEWEN, M. A. and BUCHHEIM, H. P. 1998. Paleontology and paleoecology of the culminating phase of Eocene fossil lake, Fossil Butte National Monument, Wyoming. *National Park Service Paleontological Research*, **3**, 73–80.

MANNING, P. L., EDWARDS, N. P., BERGMAN, U., ANNE, J., SELLERS, W. I., VAN VEELEN, A., SOKARAS, D., EGERTON, V. M., ALONSO-MORI, R., IGNATYEV, K., VAN DONGEN, B. E., WAKAMATSU, K., ITO, S., KNOLL, F. and WOGELIUS, R. A. 2019. Pheomelanin pigment remnants mapped in fossils of an extinct mammal. *Nature Communications*, **10**, 2250.

MCNAMARA, M. E., BRIGGS, D. E. G., ORR, P. J., FIELD, D. J. and WANG, Z. 2013. Experimental maturation of feathers: implications for reconstructions of fossil feather colour. *Biology Letters*, **9**, 20130184.

—— VAN DONGEN, B. E., LOCKYEAR, N. P., BULL, I. D. and ORR, P. J. 2016. Fossilization of melanosomes via sulfurization. *Palaeontology*, **59**, 337–350.

NAPPI, A. J. and CHRISTENSEN, B. M. 2005. Melanogenesis and associated cytotoxic reactions: applications to insect innate immunity. *Insect Biochemistry & Molecular Biology*, **35**, 443–459.

OAKLEY, T. H. and SPEISER, D. I. 2015. How complexity originates: the evolution of animal eyes. *Annual Review of Ecology, Evolution & Systematics*, **46**, 237–260.

PEDERSEN, G. K. and BUCHARDT, B. 1996. The calcareous concretions (cementsten) in the Fur formation (Paleogene, Denmark): isotopic evidence of early diagenetic growth. *Bulletin of the Geological Society of Denmark*, **43**, 78–86.

RAVEL, B. and NEWVILLE, M. 2005. Athena, Artemis, Hephaestus: data analysis for X-ray absorption spectroscopy using IFEFFIT. *Journal of Synchrotron Radiation*, **12**, 537–541.

ROGERS, C. S., ASTROP, T. I., McNAMARA, M. E., WEBB, S. M., ITO, S. and WAKAMATSU, K. 2019. Synchrotron-X-ray absorption spectroscopy of melanosomes in vertebrates and cephalopods: implications for the affinity of *Tullimonstrum*. *Proceedings of the Royal Society B*, **286**, 20191649.

—— WEBB, S. M. and McNAMARA, M. E. 2020. Data from: Synchrotron-X-ray fluorescence analysis reveals diagenetic alteration of fossil melanosome trace metal chemistry. *Dryad Digital Repository*. https://doi.org/10.5061/dryad.r7sqv9s7q

ROSSI, V., McNAMARA, M. E., WEBB, S. M., ITO, S. and WAKAMATSU, K. 2019. Tissue-specific geometry and chemistry of modern and fossilized melanosomes reveal internal anatomy of extinct vertebrates. *Proceedings of the National Academy of Sciences*, **116**, 17880–17889.

—— WEBB, S. M. and McNAMARA, M. E. 2020. Hierarchical biota-level and taxonomic controls on the chemistry of fossil melanosomes revealed using synchrotron X-ray fluorescence. *Scientific Reports*, **10**, 8970.

SCHROETER, E. R., DEHART, C. J., CLELAND, T. P., ZHENG, W., THOMAS, P. M., KELLEHER, N. L., BERN, M. and SCHWEITZER, M. H. 2017. Expansion for the *Brachylophosaurus canadensis* collagen I sequence and additional evidence of the preservation of Cretaceous protein. *Journal of Proteome Research*, **16**, 920–932.

SCHWEITZER, M. H., SUO, Z., RECEP, A., ASARA, J. M., ALLEN, M. A., ARCE, F. T. and HORNER, J. R. 2007. Analysis of soft tissue from *Tyrannosaurus rex* suggests the presence of protein. *Science*, **316**, 277–280.

—— ZHENG, W., CLELAND, T. P. and BERN, M. 2013. Molecular analyses of dinosaur osteocytes support the presence of endogenous molecules. *Bone*, **52**, 414–423.

STANKIEWICZ, A. R., BRIGGS, D. E. G., MICHELS, R., COLLINSON, M. E., FLANNERY, M. B. and EVERSHED, R. P. 2000. Alternative origin of aliphatic polymer in kerogen. *Geology*, **28**, 559–562.

WEBB, S. M. 2011. The microanalysis toolkit: x-ray fluorescence image processing software. *AIP Conference Proceedings*, **1365**, 196–199.

WOGELIUS, R. A., MANNING, P. L., BARDEN, H. E., EDWARDS, N. P., WEBB, S. M., SELLERS, W. I., TAYLOR, K. G., LARSON, P. L., DODSON, P., YOU, H., DA-QING, L. and BERGMANN, U. 2011. Trace metals as biomarkers for eumelanin pigment in the fossil record. *Science*, **333**, 1622–1626.